INDERSCIENCE PUBLISHERS
Linking academia, business and industry through research

International Journal of Surface Science and Engineering

ISSN online: 1749-7868 - ISSN print: 1749-785X
https://www.inderscience.com/ijsurfse

Investigation on the transient asperity contact behaviours of water-lubricated bearing under start-stop cycle

Tianyou Yang, Guo Xiang, Cheng Wang, Liwu Wang, Hang Jia, Jiaxu Wang

DOI: 10.1504/IJSURFSE.2024.10067455

Article History:

Received:	20 April 2024
Last revised:	02 June 2024
Accepted:	22 June 2024
Published online:	04 March 2025

Investigation on the transient asperity contact behaviours of water-lubricated bearing under start-stop cycle

Tianyou Yang and Guo Xiang*

School of Mechanical and Power Engineering,
Chongqing University of Science and Technology,
Chongqing 401331, China
and
College of Mechanical and Vehicle Engineering,
Chongqing University,
Chongqing, 400044, China
Email: 1635271628@qq.com
Email: guoxiang@cqust.edu.cn
*Corresponding author

Cheng Wang and Liwu Wang

College of Mechanical and Vehicle Engineering,
Chongqing University,
Chongqing, 400044, China
Email: 1635271628@qq.com
Email: 1411003575@qq.com

Hang Jia

School of Mechanical and Power Engineering,
Chongqing University of Science and Technology,
Chongqing 401331, China
Email: 1317304955@qq.com

Jiaxu Wang

School of Mechanical and Power Engineering,
Chongqing University of Science and Technology,
Chongqing 401331, China
and
College of Mechanical and Vehicle Engineering,
Chongqing University,
Chongqing, 400044, China
Email: profwjx@qq.com

Abstract: The main purpose of this study is to assess the transient lubrication performances and dynamic behaviours of water-lubricated bearings during start-stop cycle based on the numerical prediction. The transient mixed

lubrication model coupled with dynamic equation during start-stop cycle is established, in which the asperity contacts, and elastic deformation are considered. The effectiveness of the present numerical simulation is verified by the comparisons with the published test results. Based on the numerical study, the transient asperity contacts and dynamic behaviours under different radial clearances and acceleration time are revealed. The results demonstrate that at the initial and end time during the start-stop cycle; the asperity contact is more serious. That is because the hydrodynamic water film is not quite formed at the initial start-up period and at the shut-down period the hydrodynamic water film is going to disappear. As a result, during this period, the external load is mainly shared by the contact load. Especially when the radial clearance is small, the asperity contact is more serious. In addition, under longer acceleration time, the journal trajectory shows better consistency of the start-up and shut-down conditions.

Keywords: start-stop cycle; water-lubricated bearing; asperity contact; mixed lubrication.

Reference to this paper should be made as follows: Yang, T., Xiang, G., Wang, C., Wang, L., Jia, H. and Wang, J. (2025) 'Investigation on the transient asperity contact behaviours of water-lubricated bearing under start-stop cycle', *Int. J. Surface Science and Engineering*, Vol. 19, No. 1, pp.76–94.

Biographical notes: Tianyou Yang is a PhD student in College of Mechanical and Vehicle Engineering, Chongqing University. His research interests include fluid-solid-thermal coupled performances, wear performance and optimisation of journal bearing, and water-lubricated bearing tribology.

Guo Xiang is an Assistant Professor in School of Mechanical and Power Engineering, Chongqing University of science and technology. His research interests include lubrication and wear simulation, tribo-dynamic modelling, friction-induced vibration and water lubricated bearing.

Cheng Wang is a PhD student in College of Mechanical and Vehicle Engineering, Chongqing University. His research interests include wear performance and optimisation of journal bearing, and water-lubricated bearing tribology.

Liwu Wang is a PhD student in College of Mechanical and Vehicle Engineering, Chongqing University. His research interests include vibration performance, wear performance and optimisation of journal bearing, and water-lubricated bearing tribology.

Hang Jia is an Assistant Professor in School of Mechanical and Power Engineering, Chongqing University of science and technology. His research interests include lubrication and wear simulation, friction-induced vibration and water lubricated bearing.

Jiaxu Wang is a Professor in College of Mechanical and Vehicle Engineering, Chongqing University. His research interests include lubrication and wear simulation, tribo-dynamic modelling, friction-induced vibration and water lubricated bearing.

1 Introduction

Water lubricated journal bearing, because of its environmental friendly, energy saving and noise reduction, is widely used in underwater vehicle (Deng, 2024; Deng et al., 2019; Yan et al., 2017). Due to the low viscosity of the water, the thickness of the water film between the journal and the bearing is usually too small to provide sufficient load capacity. As a result, water-lubricated bearing is usually worked in mixed lubrication condition or even boundary lubrication condition (Anil et al., 2017; Chinnusamy et al., 2024; Deng, 2023; Yao et al., 2023). Especially during the start-up and shut-down cycle, the hydrodynamic force yielded by the water film is typically insufficient to support the external load, which leads to the serious asperity contact. Therefore, it is of great significance to study the tribo-dynamic performances of water lubricated bearing during the start-stop cycle.

Earlier, Mokhtar et al. (1977a, 1977b) studied the starting behaviour of plain, hydrodynamic journal bearings during starting and stopping under a steady load. The results show that the sliding wear typically occurs during start-up due to the excessive asperity contact and the hydrodynamic film is formed in a very short time. They measured the journal trajectory and the wear behaviour of the journal bearing at the start-up stage and argued the journal bearing was more prone to sliding wear at the start-up stage compared with the stopping stage. Monmousseau and Fillon (2000) investigated the transient thermoelastohydrodynamic behaviour of a tilting-pad journal bearing during start-up exposed to severe operating conditions. Later, Bouyer and Fillon (2011) conducted several experiments to understand the mechanisms occurring during the transition between mixed lubrication and hydrodynamic lubrication. Cristea et al. (2017, 2011) experimentally measured the fluid pressure, temperature fields, friction torque and oil flow rate of the circumferential groove journal bearing during the start-up time. The results showed that the pressure field is established faster than the temperature field. Cui et al. (2020, 2018) found that the surface roughness has an important effect on the transient characteristics of the bearing during the initial period of startup. That means the asperity contact cannot be ignored during the start-up periods. König et al. (2021) proposed some approaches for the prediction of friction in sliding bearings subjected to start-stop operation and results showed that the actual distribution and position of surface roughness played a great role in the frictional losses in sliding bearings during start-stop operation.

Recently, Guo et al. (2023), Tang et al. (2024), Xiang et al. (2021) and Yang et al. (2024) numerically investigated the tribo-dynamic lubrication performance of water-lubricated bearing during the start-up condition. The influence of wear and imperfect journal were considered. They declared that a relatively small accelerating time is beneficial to reduce the asperity contact time. Liang et al. (2022) assessed the effect of sea wave shock on the start performance of water-lubrication bearing. They found that both the amplitude and the time of sea wave shock have a significant influence on the lubrication performance during start-up condition. Cao et al. (2022) proposed a thermo-elasto-hydrodynamic approach to analyse the transient lubrication characteristics of a bidirectional thrust bearing during start-up. However, the tribo-dynamic performance of water-lubricated bearings during start-stop cycles are still lacked, especially the dynamic behaviours during the shut-down process.

The main purpose of the present study is to reveal the transient tribo-dynamic and asperity contact performance of water-lubricated bearings during start-stop cycle using a

numerical model. Based on the simulations, the effect of the radial clearance on the transient tribo-dynamic and asperity contact behaviour of the water-lubricated bearing under start-stop cycle has been investigated. Furthermore, the results under different acceleration and deceleration time have been compared. The results show that smaller radial clearance will lead to more serious asperity contact.

2 Mathematical model

2.1 Dynamic equations

The journal trajectory is excited by the transient hydrodynamic load, contact load and friction load, and the journal will be displaced in both horizontal and vertical directions. In the presented study, the following rotor dynamic equation was used to assess the journal dynamic behaviour.

$$\begin{cases} m_J\zeta'' = W + F_{fric\zeta}(t) - F_{h\zeta}(t) - F_{c\zeta}(t) + m_J\omega^2 r\cos\left(\dfrac{2\pi\omega}{60}t\right) \\ m_J\kappa'' = F_{h\kappa}(t) + F_{c\kappa}(t) + F_{fric\kappa}(t) + m_J\omega^2 r\sin\left(\dfrac{2\pi\omega}{60}t\right) \end{cases} \tag{1}$$

where m_J is the mass of the rotor; $F_h(t)$, $F_c(t)$ and $F_{fric}(t)$ are the transient hydrodynamic load, contact load and friction load, respectively; r is unbalance eccentricity of the rotor.

Figure 1 Bearing configuration and coordinate system (see online version for colours)

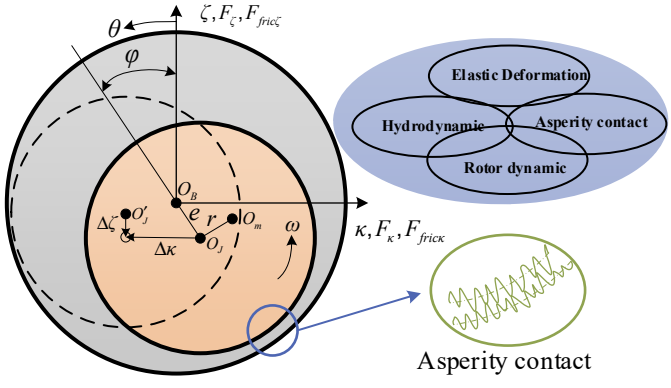

2.2 Acceleration and deceleration model

The function of velocity to time is expressed as follows. The full operating time can be divided into four periods, the acceleration time, the steady time, the deceleration time and the end time. During the acceleration time, the linear acceleration mode is adopted.

$$\begin{cases} v_{J\theta}(t) = v_m t / t_a & 0 \le t < t_a \\ v_{J\theta}(t) = v_m & t_a \le t < 2t_a \\ v_{J\theta}(t) = v_m (3t_a - t)/t_a & 2t_a \le t < 3t_a \\ v_{J\theta}(t) = 0 & 3t_a \le t \le 4t_a \end{cases} \tag{2}$$

where t_a is the acceleration time and is equal to the deceleration time; v_m is the linear velocity of the rotor under steady running process.

2.3 Transient hydrodynamic model

During the start-stop cycle, the asperity contact will occur and the water-lubricated bearing is working under the mixed lubrication condition. In this present study, the average Reynolds equation developed by Patir and Cheng (1978) is applied here to calculate for the transient hydrodynamic force considered with asperity contact and roughness effect.

$$\frac{\partial}{R_B{}^2 \partial\theta}\left(\phi_\theta \frac{h^3}{12\eta}\frac{\partial p_h}{\partial\theta}\right) + \frac{\partial}{\partial z}\left(\phi_z \frac{h^3}{12\eta}\frac{\partial p_h}{\partial z}\right) = \frac{\omega}{2}\left(\phi_c \frac{\partial h}{\partial\theta} + \sigma\frac{\partial \phi_s}{\partial\theta}\right) + \frac{\partial h}{\partial t} \tag{3}$$

where h is the lubrication gap, η is viscosity of water, respectively; ϕ_θ and ϕ_z (Patir and Cheng, 1978) are the flow factors in the circumferential and axial directions, respectively; ϕ_s (Patir and Cheng, 1978) and ϕ_c (Wu and Zheng, 1989) are the shear and contact factors, respectively; σ is the composite surface roughness; p_h is the hydrodynamic pressure of the water. The Reynolds boundary condition is used in the current simulation.

$$\begin{cases} p_{hJ}(\theta, 0) = p_{hJ}(\theta, L) = 0 & (J = 0, h\zeta, h\kappa, h\zeta', h\kappa') \\ p_{hJ}(\theta_0, z) = 0, \partial p_{hJ}(\theta_0, z)/\partial\theta = 0 & (J = 0, h\zeta, h\kappa, h\zeta', h\kappa') \end{cases} \tag{4}$$

2.4 Transient contact model

Due to the low viscosity of the water, the journal and the bearing cannot be completely separated by the water film especially when the rotation speed is low during the start-stop cycle. The asperity contact between journal and bearing should not be ignored for a more accurate assess of the tribo-dynamic behaviours during the start-stop cycle. The transient asperity contact model developed by Greenwood and Tripp (1970) is used here to obtain the contact pressure, which can be written as:

$$p_c(\theta, z, t) = KE^* F(H(t)) \tag{5}$$

where K is a constant depending on the surface parameters, which can be calculated by

$$K = \frac{16\sqrt{2}\pi}{15}(\sigma\beta D)^2\sqrt{\frac{\sigma}{\beta}} \tag{6}$$

where D and β are the density and the curvature radius of asperities, respectively. The time-varying contact load can be calculated as follows:

$$F(H(t))=\begin{cases}4.4086\times10^{-5}(4-H(t))^{6.804} & if\ H(t)<4\\ 0 & if\ H(t)\geq 4\end{cases} \tag{7}$$

2.5 Transient lubrication gap

The transient lubrication gap considering of elastic deformation of the bearing can be expressed as:

$$h(\theta, z, t)=C(1+\varepsilon(t)\cos(\theta-\varphi(t)))+\delta_{BE}(\theta, z, t) \tag{8}$$

where $\varepsilon(t)$ and $\varphi(t)$ are the transient eccentricity ratio and the attitude angle, respectively; δ_{BE} is the elastic deformation.

2.6 Load capacity

The transient hydrodynamic load can be obtained by integration of the water film pressure, as follows:

$$\begin{cases}F_{h\kappa}(t)=\int_0^L\int_0^{2\pi} p_h(\theta, z, t)R_B\sin(\theta)d\theta dz\\ F_{h\zeta}(t)=-\int_0^L\int_0^{2\pi} p_h(\theta, z, t)R_B\cos(\theta)d\theta dz\end{cases} \tag{9}$$

where $F_{h\kappa}$ and $F_{h\zeta}$ are the vertical and horizontal hydrodynamic forces, respectively. Under the mixed lubrication regime, the friction force is composed of the contact shear force and the water film shear force, which can be given by:

$$\begin{cases}F_{fric\kappa}(t)=\int_0^L\int_0^{2\pi}\left(\frac{\eta\omega R_B}{h(t)}+\frac{h(t)}{2}\frac{\partial p_h(t)}{R_B\partial\theta}+\mu_c p_c(t)\right)\cos(\theta)d\theta dz\\ F_{fric\zeta}(t)=\int_0^L\int_0^{2\pi}\left(\frac{\eta\omega R_B}{h(t)}+\frac{h(t)}{2}\frac{\partial p_h(t)}{R_B\partial\theta}+\mu_c p_c(t)\right)\sin(\theta)d\theta dz\end{cases} \tag{10}$$

2.7 Simulation procedure

Figure 2 shows the flow chart of the transient mixed lubrication analysis for water-lubricated bearing during start-up and shut-down periods. The steady equations are solved first to initial the lubrication gap and start the transient start-up and shut-down process. The transient average Reynolds equation is solved using the finite difference method (FDM), and the convergence accuracy is set to be 1.0×10^{-5} while the mesh density is 160 for circumferential direction and 21 for axial direction. After obtained the transient hydrodynamic force, contact force and friction force, the rotor dynamic equation can be solved using Runge-Kuta method with second order accuracy. Then the journal centre position and the lubrication gap can be updated to calculate for the next timestep with the updating velocity of the rotor until reaching the given time. In this current simulation, the acceleration time is set to be 0.25 s, and the total time is fourth time to the

acceleration time while the step time is set to be 0.5 μs. The material of the bearing is polymer and the journal is 45-steel. Other simulation parameters used in the present study are listed in Table 1.

Figure 2 Flow chart of the calculation procedure (see online version for colours)

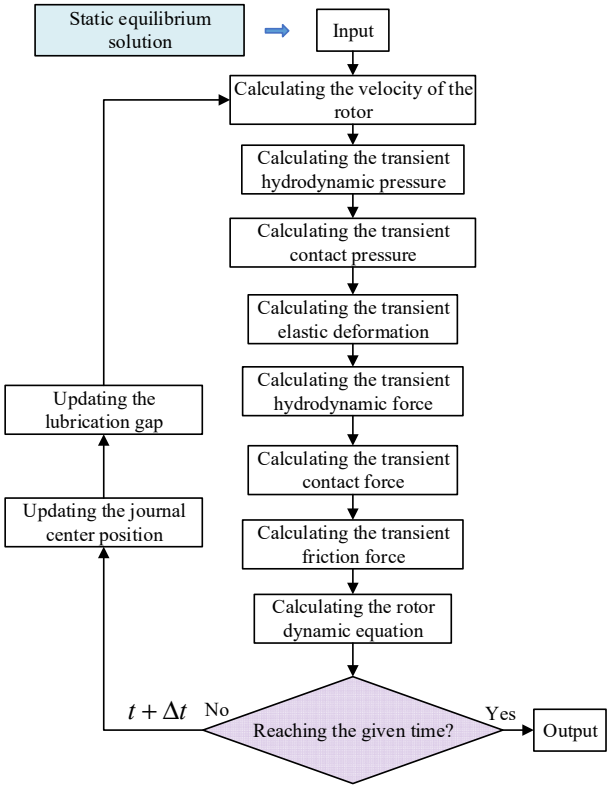

Table 1 Basic parameters of water-lubricated bearing system

Parameter	*Value*	*Parameter*	*Value*
Inner radius/R_B	22.5 mm	Journal roughness/σ_J	0.2 μm
Outer radius/R_O	25 mm	Journal density/ρ_J	7,800 kg/m^3
Bearing width/L	40 mm	Journal elastic modulus/E_J	210 GPa
Clearance/C	0.05 mm	Journal Poisson ratio/v_J	0.3
Bearing hardness/H_B	0.3 GPa	Friction coefficient/μ_c	0.1
Bearing density/ρ_B	1,300 kg/m^3	Bearing roughness/σ_B	0.6 μm
Bearing elastic modulus/E_B	2.32 GPa	Bearing Poisson ratio/v_B	0.327
Water density/ρ_W	1,000 kg/m^3	Contact parameter/$\sigma\beta$D	0.04
Water viscosity/η_W	0.001 Pa.s	Contact parameter/σ/β	0.01
Acceleration/t_a	0.25 s	Step time/Δt	0.5 μs
External load/W	1,000 N	Steady rotation speed/ω	1,000 rpm

3 Results and discussion

3.1 Model validation

In order to validate the accuracy of the present numerical model, the simulation results are compared to the published test results given by Mokhtar et al. (1977a, 1977b). The test parameters of journal bearing are listed in Table 2. As shown in Figure 3(a), the asperity contact time under different external load of simulation results obtained by the present mathematical model shows a good agreement to the test result given by Mokhtar et al. (1977a, 1977b). The journal trajectories of simulation and test results are plotted in Figure 3(b). During the start-up period, the journal is gradually lifted and separate from the bearing to form hydrodynamic film. Therefore, the comparisons plotted in Figure 3 demonstrate that the present mathematical model accurately predict the tribo-dynamic behaviours for water-lubricated bearing during the start-stop cycle.

Figure 3 Verification of the tribo-dynamic performances during start-stop: (a) rotor trajectory, (b) contact time (see online version for colours)

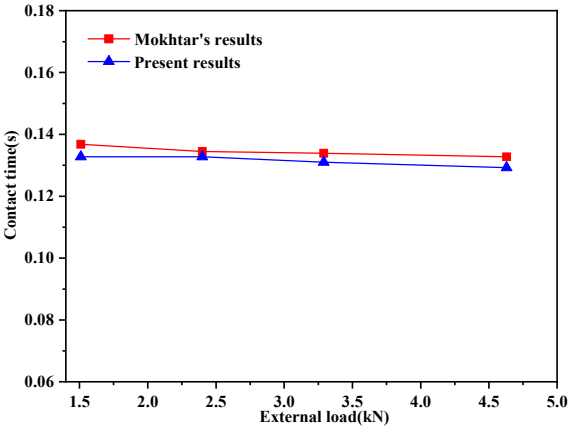

(a)

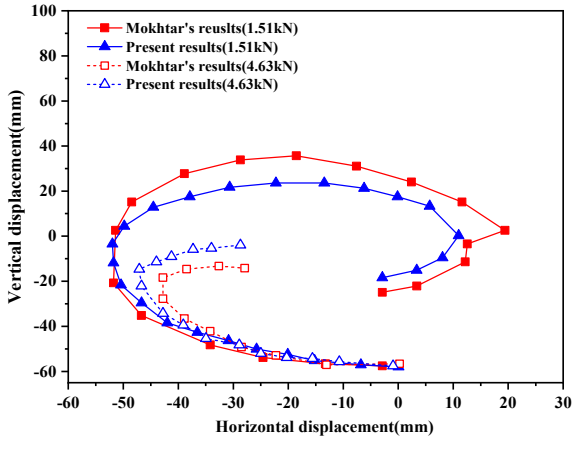

(b)

Table 2 Tested parameters of journal bearing given by Mokhtar et al. (1977a, 1977b)

Parameters	*Value*	*Parameters*	*Value*
Bearing inner radius	37.326 mm	Bearing material	Lead-bronze alloy
Bearing width	76.2 mm	Acceleration time	0.3 s
Radius clearance	0.12 mm	Journal roughness	0.12 μm
Rotation speed	850 rpm	Bearing roughness	1.473 μm
Journal material	Steel	Viscosity of the oil	0.074 Pa s

Figure 4 (a) Acceleration and deceleration model, (b) Journal trajectory, (c) Hydrodynamic and contact load, (d) Maximum fluid pressure and contact pressure (see online version for colours)

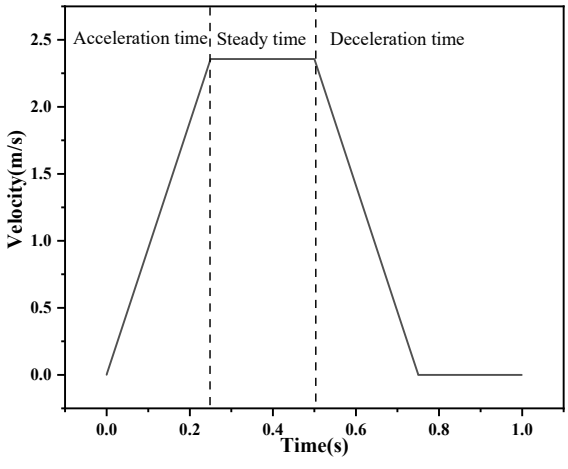

(a)

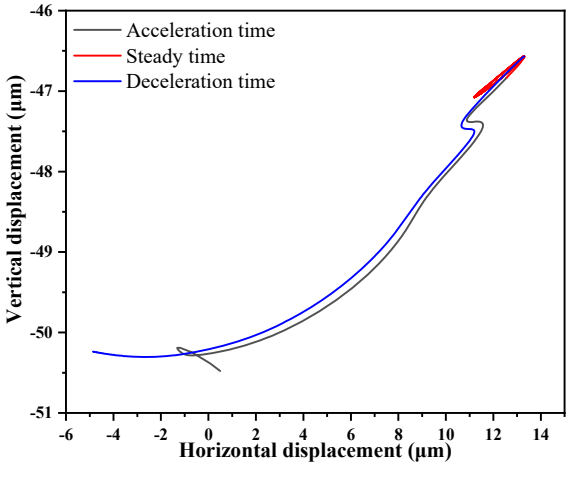

(b)

Figure 4 (a) Acceleration and deceleration model, (b) Journal trajectory, (c) Hydrodynamic and contact load, (d) Maximum fluid pressure and contact pressure (continued) (see online version for colours)

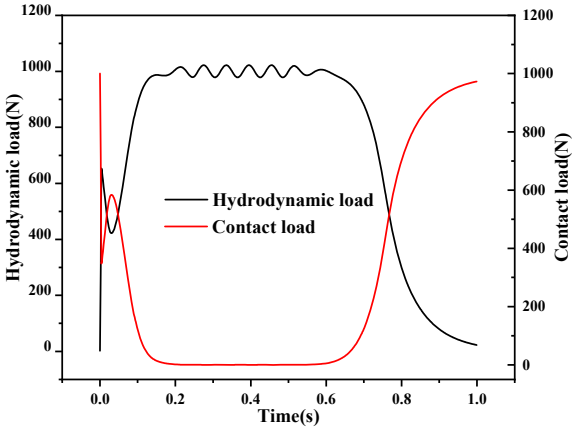

(c)

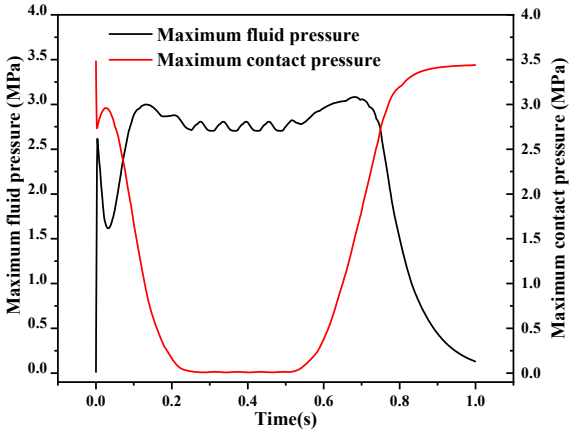

(d)

3.2 Transient performance during start-up and shut-down

The change of velocity over time is shown in Figure 4(a). It can be seen that the whole process can be divide into acceleration time (start-up), steady time and deceleration time(shut-down). At the start-up instant, the rotor will move into the opposite direction of the rotational speed as shown in Figure 4(b), which is due to the transient large horizontal friction force in the initial time of the start-up. During the start-up period, the vertical displacement is gradually smaller that means the rotor is gradually raised to generate sufficient hydrodynamic force. During the shut-down period, the rotor will gradually move to the initial position. During this period, the dynamic pressure water film disappears and the contact load increases. The variation of hydrodynamic load and contact load during the start-stop cycle is illustrated in Figure 4(c). Even the acceleration time is not quite over, the hydrodynamic is dominant to share the external load. What's

more, during the shut-down condition, the fluid pressure will not disappear immediately, but will last for a period of time as shown in Figure 4(d). What's more, the asperity contact mainly appeared during the initial time of start-up period and the end time of shut-down period. Figure 5(a) gives the distribution of fluid pressure of different time step. The fluid pressure area gradually expanded during the start-up period while the contact pressure area shrank as shown in Figures 5(a) and 5(b). During the shut-down period, the result was the opposite. The fluid pressure area gradually disappeared while the contact pressure area raised. In addition, due to the horizontal movement of the journal during the start-stop cycle, the concentrated area along the circumferential direction of the fluid pressure and contact pressure is changed of different timestep.

Figure 5 The distribution during different time, (a) fluid pressure, (b) contact pressure (see online version for colours)

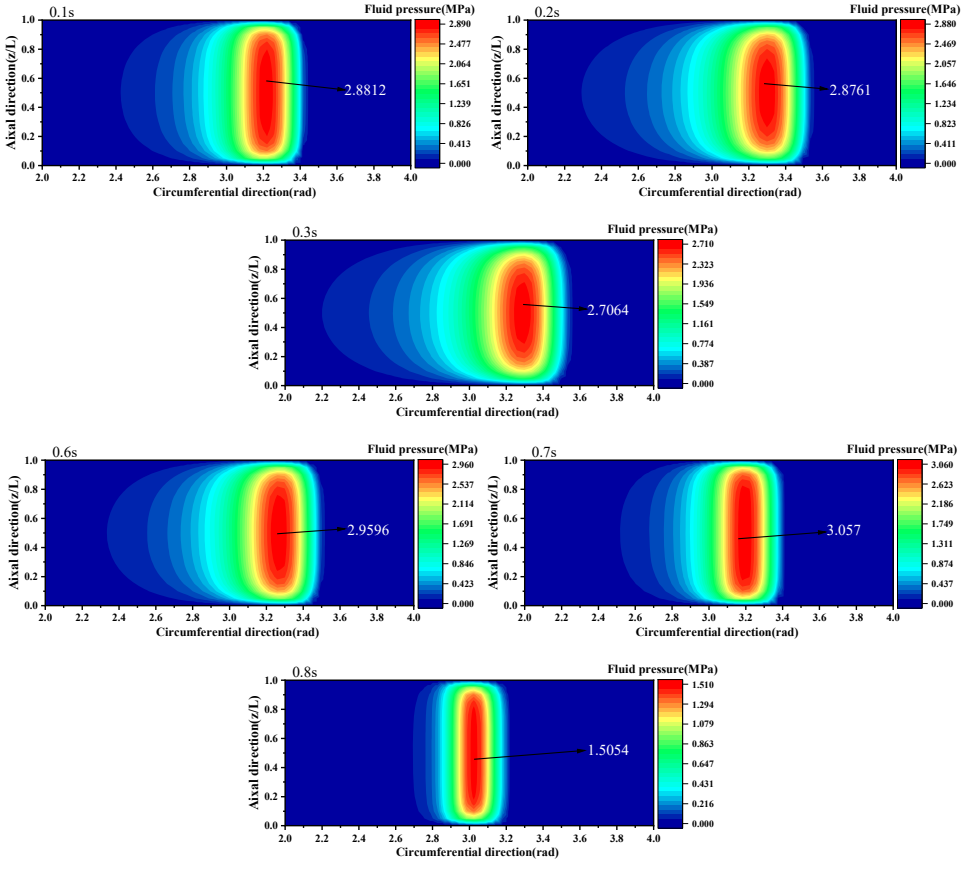

(a)

Figure 5 The distribution during different time, (a) fluid pressure, (b) contact pressure (continued) (see online version for colours)

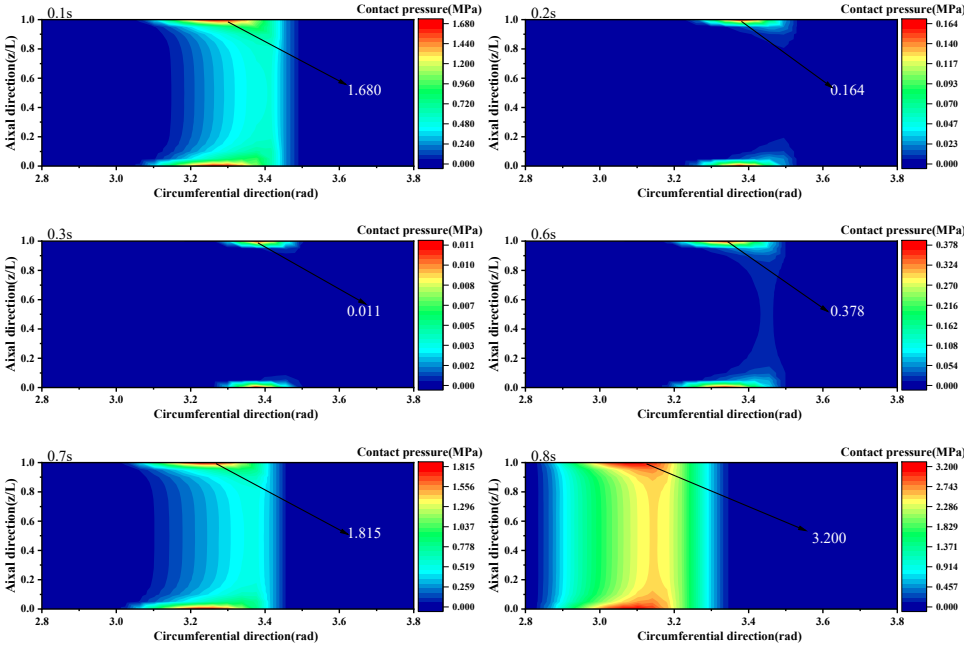

(b)

Figure 6 Journal trajectory under different radial clearances

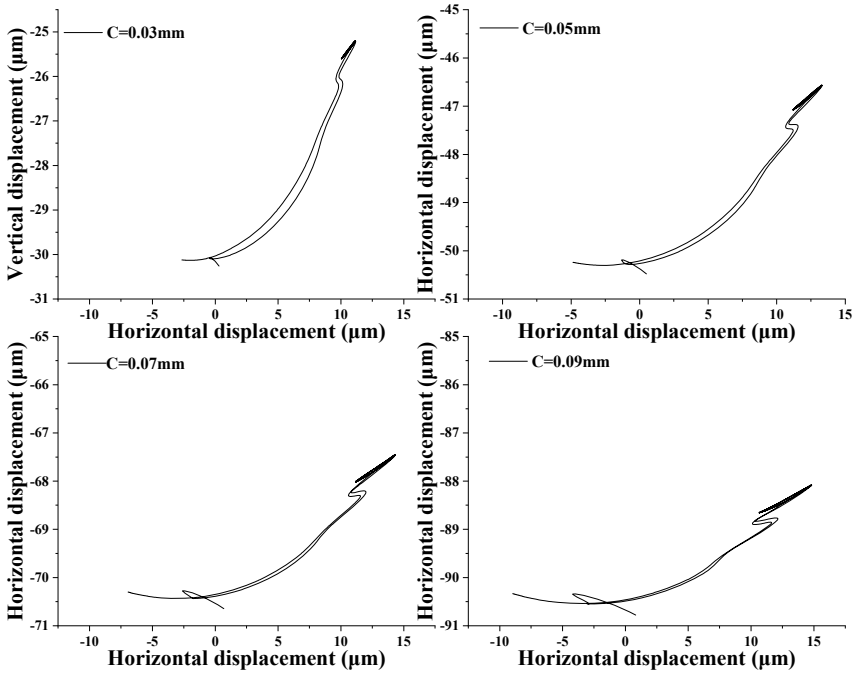

Figure 7 (a) Hydrodynamic and contact load under different radial clearances, (b) Maximum fluid pressure and contact pressure under different radial clearances (see online version for colours)

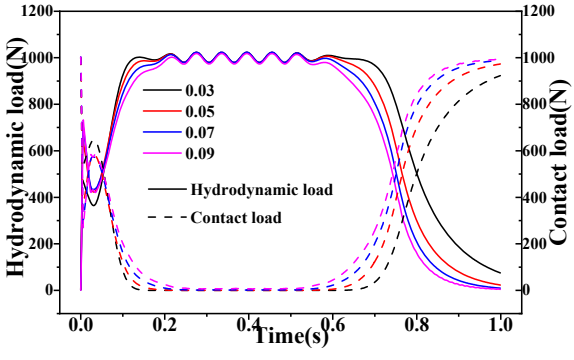

(a)

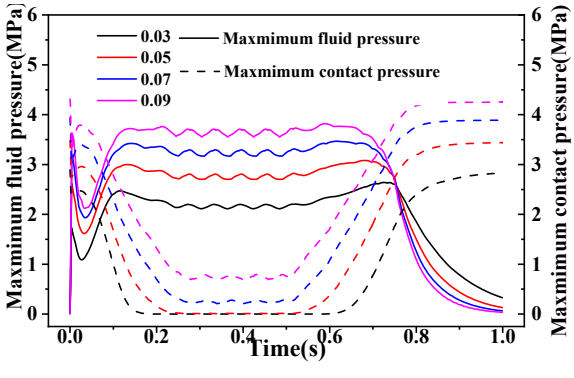

(b)

3.3 Parameters evolution

3.3.1 Effect of radial clearance

Figure 6 exhibits the axis orbit of the journal under different radial clearance. It can be seen that the horizontal displacement is small and the vertical displacement is bigger under smaller radial clearance. This is because under the same external load, the smaller eccentricity can provide enough hydrodynamic load under smaller radial clearance. In addition, during the start-up condition, the dynamic water film forms faster. Enough hydrodynamic can be formed in a relatively short start time as shown in Figure 7(b). During the shut-down period, the fluid pressure lasts for a longer time under smaller radial clearance. And, under smaller radial clearance, the maximum contact pressure significant decreased during the whole start-stop cycle.

Figure 8 Journal trajectory under different acceleration time

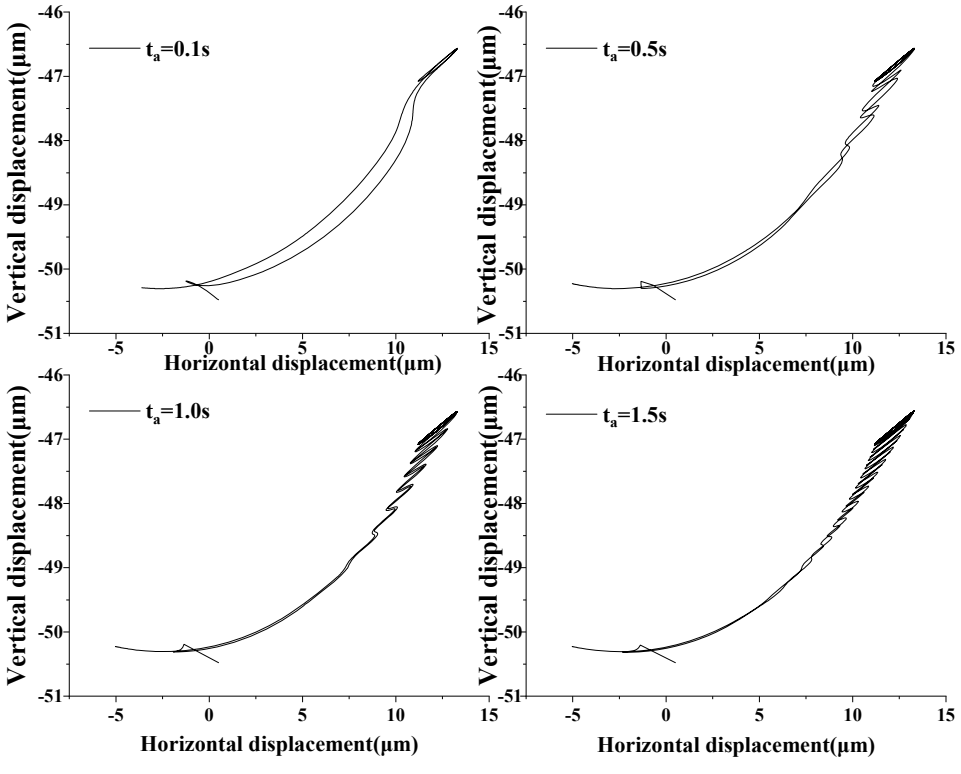

3.3.2 Effect of acceleration time

Figure 8 compared the axis orbit of the journal under different acceleration times, it can be seen that journal trajectory is roughly the same. When the acceleration time is longer, the dynamic response is more stable. As a result, the journal trajectory under start-up condition is more consistent with journal trajectory under shut-down periods compared to the shorter acceleration time. The maximum fluid pressure and contact pressure is almost the same under different acceleration time during the whole start-stop cycle as shown in Figure 9(b). In the initial phase of start-up, the asperity contact will last longer time under the longer acceleration time. In order to avoid the wear caused by the asperity contact, the acceleration time should not be too long. In addition, it can be observed from Figure 9 that at the beginning of start-up there are a sudden increase in the hydrodynamic load and a sudden decrease in the contact load (‘friction drag’ effect).

Figure 9 (a) Hydrodynamic and contact load under different acceleration time, (b) Maximum fluid pressure and contact pressure under different acceleration time (see online version for colours)

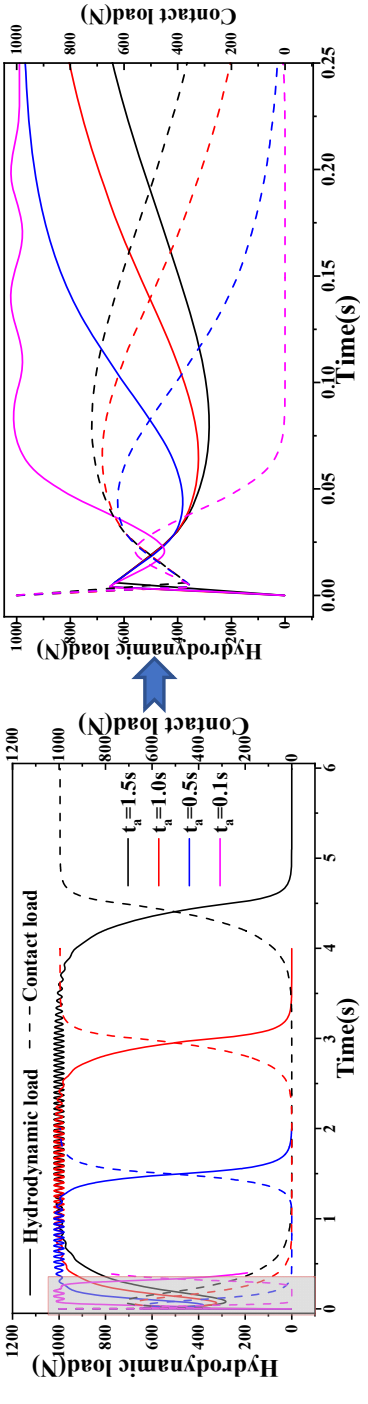

(a)

Figure 9 (a) Hydrodynamic and contact load under different acceleration time, (b) Maximum fluid pressure and contact pressure under different acceleration time (continued) (see online version for colours)

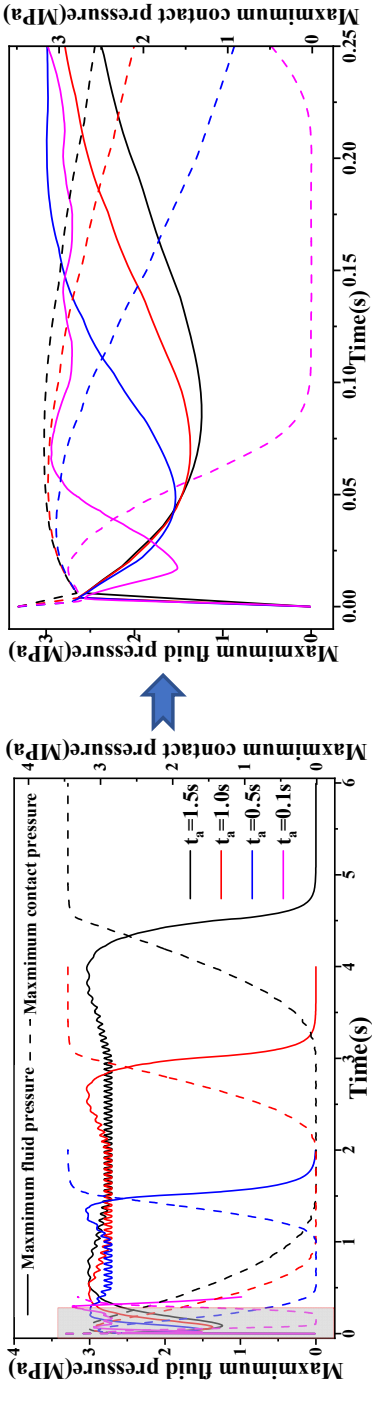

(b)

4 Conclusions

In this study, the transient asperity contact behaviours and dynamic responses of water-lubricated bearing during start-stop cycle are investigated according to the numerical simulation. In addition, the effects of radial clearances and acceleration time on transient mixed lubrication performances are compared. The following conclusions can be summarised:

1 In the initial time of start-up, the hydrodynamic water film has not yet fully formed and is going to disappear in the end time of the shut-down. As a result, during these periods the external load is mainly shared by the contact force caused by the asperity contact.

2 Under larger radial clearance, the asperity contact is more serious as the maximum contact pressure is significant larger during the whole start-stop cycle.

3 The journal trajectory shows better consistency during the start-up and shut-down condition under longer acceleration time. And the asperity contact lasts for a longer time under longer acceleration time.

Data availability

The data that support the findings of this study are available from the corresponding author upon reasonable request.

References

Anil, P.M., Kumar, R. and Sethuramiah, A. (2017) 'Effect of initial roughness and oxidation on the running-in wear of machined surfaces under dry sliding', *International Journal of Surface Science and Engineering*, Vol. 11, No. 7, pp.45–64, https://doi.org/10.1504/IJSURFSE.2017.082954.

Bouyer, J. and Fillon, M. (2011) 'Experimental measurement of the friction torque on hydrodynamic plain journal bearings during start-up', *Tribology International*, Vol. 44, No. 7, pp.772–781, https://doi.org/10.1016/j.triboint.2011.01.008.

Cao, J., Zhai, L., Luo, Y., Ahn, S-H., Wang, Z. and Liu, Y. (2022) 'Transient thermo-elasto-hydrodynamic analysis of a bidirectional thrust bearing in start-up and shutdown processes', *Engineering Computations*, Vol. 39, No. 4, pp.1511–1533, https://doi.org/10.1108/EC-03-2021-0128.

Chinnusamy, T.R., Sivakumar, A., Raja, V.L. and Kathan, A. (2024) 'A single asperity elastic-plastic contact model with the effect of kinematic strain hardening', *International Journal of Surface Science and Engineering*, Vol. 18, No. 2, pp.149–171, https://doi.org/10.1504/IJSURFSE.2024.138507.

Cristea, A-F., Bouyer, J., Fillon, M. and Pascovici, M.D. (2011) 'Pressure and temperature field measurements of a lightly loaded circumferential groove journal bearing', *Tribology Transactions*, Vol. 54, No. 5, pp.806–823, https://doi.org/10.1080/10402004.2011.604758.

Cristea, A-F., Bouyer, J., Fillon, M. and Pascovici, M.D. (2017) 'Transient pressure and temperature field measurements in a lightly loaded circumferential groove journal bearing from startup to steady-state thermal stabilization', *Tribology Transactions*, Vol. 60, No. 6, pp.988–1010, https://doi.org/10.1080/10402004.2016.1241330.

Cui, S., Gu, L., Fillon, M., Wang, L. and Zhang, C. (2018) 'The effects of surface roughness on the transient characteristics of hydrodynamic cylindrical bearings during startup', *Tribology International*, Vol. 128, pp.421–428, https://doi.org/10.1016/j.triboint.2018.06.010.

Cui, S., Zhang, C., Fillon, M. and Gu, L. (2020) 'Optimization performance of plain journal bearings with partial wall slip', *Tribology International*, Vol. 145, p.106137, https://doi.org/10.1016/j.triboint.2019.106137.

Deng, X. (2023) 'A mixed zero-equation and one-equation turbulence model in fluid-film thrust bearings', *Journal of Tribology*, Vol. 146, No. 3, p.034101, https://doi.org/10.1115/1.4063945.

Deng, X. (2024) 'Study of temperature drop region in transitional region in fluid-film thrust bearings', *Journal of Fluids Engineering*, pp.1–43, https://doi.org/10.1115/1.4065542.

Deng, X., Gates, H., Fittro, R. and Wood, H. (2019) 'Methodology of turbulence parameter correction in water-lubricated thrust bearings', *Journal of Fluids Engineering*, Vol. 141, No. 7, p.071104, https://doi.org/10.1115/1.4042161.

Greenwood, J.A. and Tripp, J.H. (1970) 'The contact of two nominally flat rough surfaces', *Proceedings of the Institution of Mechanical Engineers*, Vol. 185, No. 1, pp.625–633, https://doi.org/10.1243/PIME_PROC_1970_185_069_02.

Guo, J., Ding, B., Wang, Y. and Han, Y. (2023) 'Co-optimization for hydrodynamic lubrication and leakage of V-shape textured bearings via linear weighting summation', *Physica Scripta*, Vol. 98, No. 12, p.125218.

König, F., Sous, C. and Jacobs, G. (2021) 'Numerical prediction of the frictional losses in sliding bearings during start-stop operation', *Friction*, Vol. 9, No. 3, pp.583–597, https://doi.org/10.1007/s40544-020-0417-9.

Liang, P., Li, X., Guo, F., Cao, Y., Zhang, X. and Jiang, F. (2022) 'Influence of sea wave shock on transient start-up performance of water-lubricated bearing', *Tribology International*, Vol. 167, p.107332, https://doi.org/10.1016/j.triboint.2021.107332.

Mokhtar, M.O.A., Howarth, R.B. and Davies, P.B. (1977a) 'Wear characteristics of plain hydrodynamic journal bearings during repeated starting and stopping', *ASLE Transactions*, Vol. 20, No. 3, pp.191–194, https://doi.org/10.1080/05698197708982833.

Mokhtar, M.O.A., Howarth, R.B. and Davies, P.B. (1977b) 'The behavior of plain hydrodynamic journal bearings during starting and stopping', *ASLE Transactions*, Vol. 20, No. 3, pp.183–190, https://doi.org/10.1080/05698197708982832.

Monmousseau, P. and Fillon, M. (2000) 'Transient thermoelastohydrodynamic analysis for safe operating conditions of a tilting-pad journal bearing during start-up', *Tribology International*, Vol. 33, No. 3, pp.225–231, https://doi.org/10.1016/S0301-679X(00)00035-9.

Patir, N. and Cheng, H.S. (1978) 'An average flow model for determining effects of three-dimensional roughness on partial hydrodynamic lubrication', *Journal of Lubrication Technology*, Vol. 100, No. 1, pp.12–17, https://doi.org/10.1115/1.3453103.

Tang, D., Xiao, K., Xiang, G., Cai, J., Fillon, M., Wang, D. and Su, Z. (2024) 'On the nonlinear time-varying mixed lubrication for coupled spiral microgroove water-lubricated bearings with mass conservation cavitation', *Tribology International*, Vol. 193, No. 1, p.109381, https://doi.org/10.1016/j.triboint.2024.109381.

Wu, C., and Zheng, L. (1989) 'An average reynolds equation for partial film lubrication with a contact factor', *Journal of Tribology*, Vol. 111, No. 1, pp.188–191, https://doi.org/10.1115/1.3261872.

Xiang, G., Wang, C., Wang, Y., Han, Y., Wang, J. and Lv, Z. (2021) 'Dynamic mixed lubrication investigation of water-lubricated bearing with unbalanced rotor during start-up', *Tribology Transactions*, Vol. 64, No. 4, pp.764–776, https://doi.org/10.1080/10402004.2021.1919341.

Yan, X., Liang, X., Ouyang, W., Liu, Z., Liu, B. and Lan, J. (2017) 'A review of progress and applications of ship shaft-less rim-driven thrusters', *Ocean Engineering* Vol. 144, pp.142–156, https://doi.org/10.1016/j.oceaneng.2017.08.045.

Yang, T., Xiang, G., Cai, J., Wang, L., Lin, X., Wang, J. and Zhou, G. (2024) 'Five-DOF nonlinear tribo-dynamic analysis for coupled bearings during start-up', *International Journal of Mechanical Sciences*, Vol. 269, p.109068, https://doi.org/10.1016/j.ijmecsci.2024.109068.

Yao, B., Xiang, G., Wang, J., Guo, J. and Nie, Y. (2023) 'Effects of wall slip on hydrodynamic performances of water-lubricated bearings under transient operating condition', *International Journal of Surface Science and Engineering*, Vol. 17, No. 2, pp.73–91, https://doi.org/10.1504/IJSURFSE.2023.130147.

Nomenclature

m_J	journal mass, kg	Δt	iteration step, s
v	linear velocity, m/s	C	radial clearance, mm
F	force, N	μ	boundary coefficient
r	unbalance eccentricity, mm	L	bearing width, mm
t_a	acceleration time, t	H_B	bearing hardness, GPa
R_B	bearing radius, mm	t	simulation time, s
ω	angular velocity, rad/s	ρ	density, kg/m^3
p	pressure, MPa	η	viscosity, Pa.s
ϕ	flow, contact, shear factors	E	elastic modulus, GPa
ε	eccentricity ratio		
δ	elastic deformation, μm	*Subscripts:*	
φ	attitude angle	θ, z	circumferential, axial
σ	surface roughness, μm	h, c	hydrodynamic, contact
β	asperity curvature radius	s	shear
D	asperity density	E	elastic
h	lubrication gap, μm	f	friction
		*	dimensionless
		$\boldsymbol{J}$	journal